

Redox Cycling Stability of Electrolyte Supported Cells

A. Glauche^a, T. Betz^a, S. Mosch^b, N. Trofimenko^b and M. Kusnezoff^b

^a Kerafol GmbH, Eschenbach i.d. Opf. 92676, Germany

^b Fraunhofer Institute for Ceramic Technologies and Systems, Dresden 01277, Germany

The electrolyte supported cells with low area specific resistance ($ASR < 0.34 \text{ } \Omega\text{cm}^2$) have been tested for redox stability in ceramic housing. It has been shown that the cells with optimized anode microstructure have no measurable resistance change in the range of mistake of used method after ten redox cycles. The small fluctuation of contact resistance between anode and current collector has been observed due to direct influence on the bonds between anode and current collector during cycling experiments.

Introduction

The robustness of SOFC systems against thermal cycling and accident events such as load throw-off, abrupt cooling down and anode oxidation because of the interrupt of fuel supply lead to requirements in respect to the thermal and redox cyclability of the stacks.

Ageing of cell properties during operation is generally not desired. The main degradation effects during the long-term operation and redox cycling take place in the anode. The reasons for the degradation of the anode in contaminant free fuel are:

- (i) Ni-agglomeration
- (ii) Mechanical stresses induced by thermal, load and redox cycles.

The Ni-agglomeration during operation and redox cycling generally can not be avoided. The agglomeration rate can be reduced to acceptable level by using ZrO_2/NiO composites.

It has been demonstrated that the long-term degradation at high current densities can be reliably solved for electrolyte supported cells operating at 850°C (1) and mainly the degradation by redox cycling is the issue which should be addressed. The goal of the carried work was to optimize the electrode (microstructure) to sustain the redox cycling.

Experimental

The lanthanum strontium manganite ($\text{La}_{0.75}\text{Sr}_{0.2}\text{MnO}_{3-x}$, uLSM), Y_2O_3 stabilized ZrO_2 (YSZ), Sc_2O_3 stabilized ZrO_2 (ScSZ) and NiO powders used in this work were supplied by different manufacturers, according to given specifications for the stoichiometry, crystalline phase, specific surface and particle size distributions.

The cathode pastes based on the uLSM/ScSZ composite were fabricated by a method which is described elsewhere in detail (1, 2).

The pastes based on the NiO-YSZ cermet powder were prepared by mixing with organic binder, organic solvent and surface active additives.

For screen printing dense 10Sc1CeSZ tapes ($50 \times 50 \times 0.150 \text{ mm}^3$) were used as substrate material. All electrochemical experiments were carried out on cells with symmetrically screen-printed cathode and anode having lateral dimensions of $40 \times 40 \text{ mm}^2$. For each experiment the cells are manufactured under similar conditions.

The cathode layer (45 μm) is composed of lanthanum strontium manganite ($\text{La}_{0.75}\text{Sr}_{0.2}\text{MnO}_{3-x}$, uLSM) and ScSZ.

The anode layer is electrochemically active cermet anode. The anode and cathode are sintered in co-firing at 1300°C.

The morphology of the studied electrodes is observed using field emission scanning electron microscopy.

All electrochemical experiments were carried out using the testing bench for MEA characterization at Fraunhofer IKTS, Dresden. The apparatus consists of a custom-built ceramic housing integrated in a furnace operated by a temperature controller enabling the temperature-time profile management up to 1100°C. Pt and Ni meshes were used as contact material for cathode and anode respectively.

The SOFC cells were characterized by impedance spectroscopy under current load at temperatures of 850-950°C in air:hydrogen/steam dual atmosphere using impedance analyzer IM6 (Zahner, Germany). The frequency was varied between 10 mHz and 100 kHz, the excitation AC voltage was fixed at 10 mV. The contributions of anode, cathode and electrolyte in the overall resistance are extracted from impedance spectra using Thales® Software (Zahner, Germany) and adequate equivalent circuit by deconvolution of impedance spectra.

Redox cycling test

The cell is first heated up to 950°C in nitrogen and then reduced. The air flow of 60 nl/h and hydrogen:steam flow of 40 nl/h are fed to the cell resulting in the open circuit voltage of 892 mV at 950°C. The current-voltage characteristics are measured at 950°C and 900°C to validate the cell performance. Afterwards the cell is cooled down to operation temperature of 850°C and the current density of 650 mA/cm². Before redox cycling treatment the cell has been operated for 200h at 650 mA/cm² to pass the activation phase reported (3).

The redox cycling takes place in-situ and includes following steps: (i) measurement of current-voltage characteristics and impedance spectra before redox cycle, (ii) shut down of steam, (iii) shut down of fuel (H_2), (iv) oxidation of anode for 3h by oxygen penetration from cathode to anode side through the leakage in the cell sealing (see Figure 1 for time dependent change of OCV during this process), (v) reduction of the anode by stepwise increase of H_2 concentration in N_2 similar to 1st reduction step at 950°C, (vi) cell activation for 12h, measurement of current-voltage characteristics and impedance spectra.

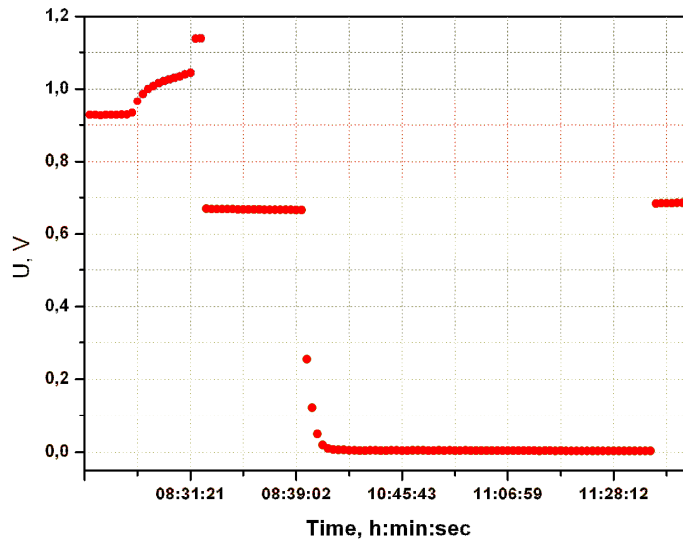


Figure 1. OCV change during the redox cycling of the cell.

To indicate the oxidation state of nickel in the anode after oxidation according to chosen procedure the analysis of anode microstructure of separate cell cooled down after oxidation step has been made (see Figure 2). It has been clearly shown that the whole nickel in the anode is fully oxidized and no metallic nickel is present after oxidation. The extension of oxidation time during this experiment causes further oxidation of nickel mesh which is only partially oxidized during step (iv).

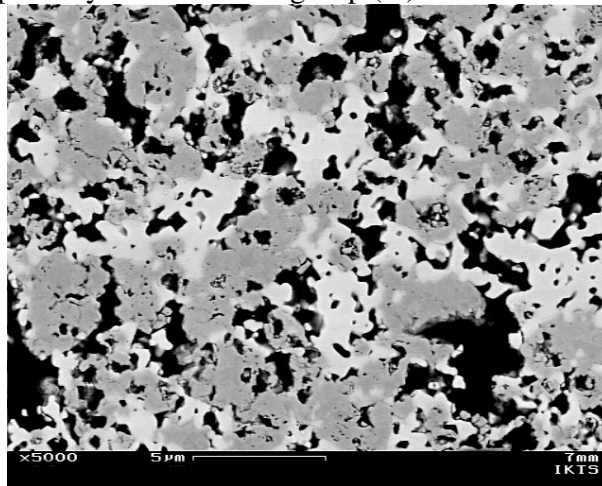


Figure 2. Anode microstructure after oxidation procedure according step (iv).

Results and Discussion

The optimization of the anode has been made to provide the intact and stable anode microstructure. The ASR at 850°C of cells manufactured using optimized technology of paste preparation, screen printing and sintering are shown in Table I. The redox cycling stability of one cell has been tested.

TABLE I. Reproducibility of ASR by different MEA lots.

MEA	temperature [°C]	j [mA/cm ²]	R _{zelle} [Ωcm ²]
579	851	725	0.286
584	851	741	0.28
603	851	700	0.297
640	851	750	0.277
687	850	747	0.278
703	851	684	0.303
549	850	715	0.292
146	853	696	0.292
145	854	723	0.289
104	850	728	0.285
693	851	650	0.317
694	851	679	0.306
697	854	667	0.308
705	854	680	0.303
641	853	699	0.302
642	855	732	0.289
678	854	716	0.291
691	853	711	0.293
695	853	727	0.284
707	856	652	0.319

Redox cycling test

The results of redox cycling of the cell in ceramic housing are shown in Fig. 3. The electrochemical activation of the cell firstly takes place during reduction process of nickel oxide to metallic nickel. The reduction temperature and procedure can directly affect the morphology of the anode because the rate of the nickel oxide reduction is affected by these parameters. To obtain the reproducible anode microstructure after reduction the same reduction procedure has been used. The oxidation / reduction cycles influence the bonds between the nickel current collector and the nickel in the anode contacting layer and in this way the contact resistance to the anode side. The main problem of redox cycling is the repeatability of electrical contact between nickel mesh and anode because the formation of contacts is directly affected by re-oxidation / reduction procedure. The properly defined and repeatable redox procedure helps to minimize this effect but can not eliminate it.

The deconvolution of impedance spectra measured after every redox cycle shows the change of different constituents of ASR values (Fig. 4). The observed changes in ASR during redox cycling are stronger in comparison to ASR scattering during thermal cycles. This scattering is explained by fluctuation of contact resistance during repetitive cycles. The obtained changes in the ASR are nevertheless very small taking into account the fluctuation of cell temperature for different measurements and scatter near to the initial ASR value.

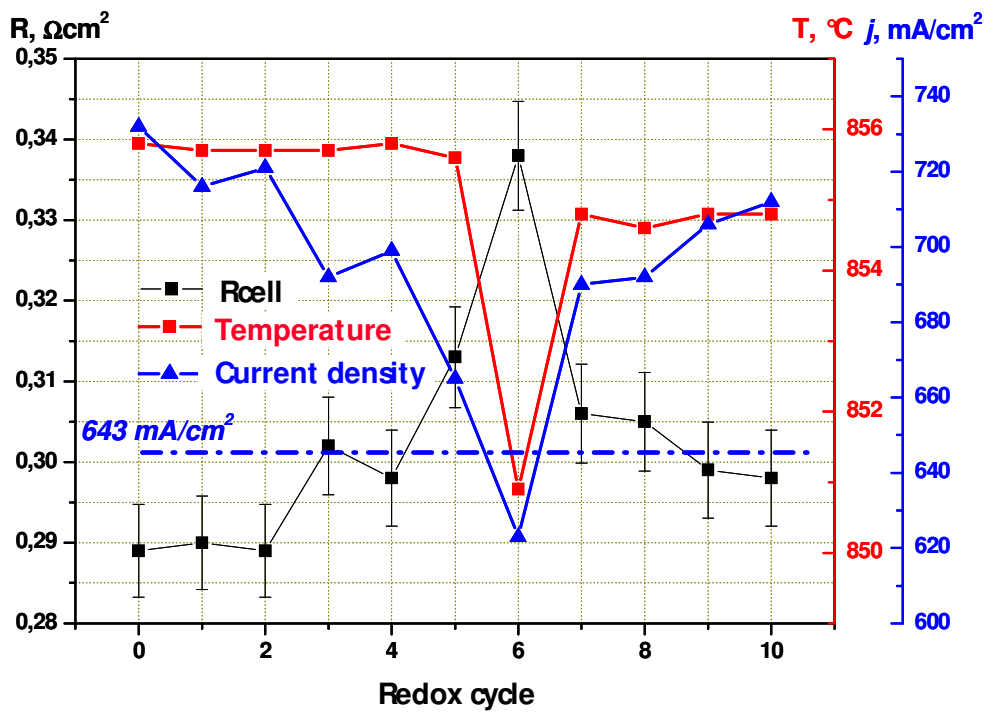


Figure 3. MEA stability during redox cycling.

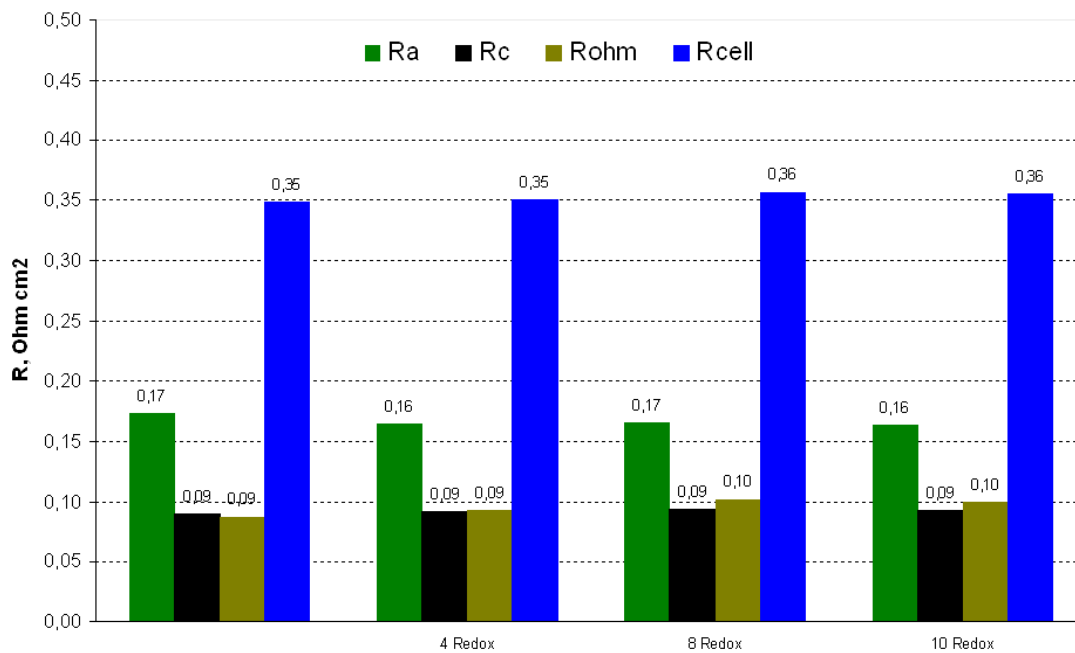


Figure 4. Constituents of ASR obtained by deconvolution of impedance spectra.

Conclusions

The redox cycling stability of electrolyte supported cells can be achieved by optimizing the anode and has been demonstrated on the newly developed cells. No regular change of cell resistance was observed after redox cycles. During measurement of the current-voltage characteristics the increase of cell temperature due to self heating at high current densities is observed. The measured ASR values correlate with cell temperature showing lower values at higher effective temperatures. The critical issue for redox cycling in stack environment is the reproducible contacting of the anode to the current collector which should be addressed by proper choice of materials and supported by stack design.

Acknowledgments

The Bavarian Ministry of Economy and Technology is kindly acknowledged for financial support under grant number NW-0509-0008.

References

1. S. Mosch, N. Trofimenko, M. Kusnezoff, T. Betz und M. Kellner: *Long-term and redox stability of electrolyte supported solid oxide fuel cells under various operating conditions*. SOFC-X, ESC Transactions, Vol. 7(1), 381–388 (2007).
2. S. Mosch, N. Trofimenko, M. Kusnezoff, T. Betz, M. Kellner, in *7th European Solid Oxide Fuel Cell Forum*, 3-7 July 2006, Lucerne, p.413, (2006)..
3. M. Kusnezoff, N. Trofimenko, S. Mosch, W. Beckert, A. Graff und F. Altmann: *Long-term stability of composite cathode at high current densities*. SOFC-X, ESC Transactions, Vol. 7 (1), 1033–1040 (2007).
4. X. Zhou, J. Templeton, Z. Nie, P. Singh, L. R. Pederson, J.W. Stevenson, *Recent Research and Development on SOFC Cathodes at PNNL*, in Proceedings of 33rd International Conference on advanced ceramics and composites (2009).